Submitted version of: J. Rossouw van der Merwe, Alejandro Fernández-Dans Goicoechea, Alexander Rügamer, Daniel Rubino, Xabier Zubizarreta, and Wolfgang Felber, “Multi-antenna snapshot receiver,” European Navigation Conference (ENC) 2019, submitted March 2019, accepted April 2018.

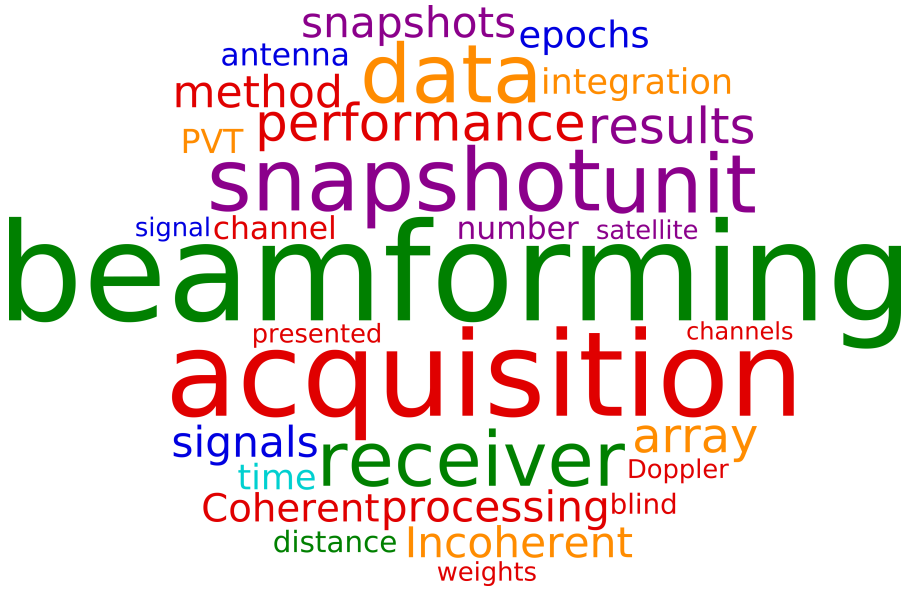

Multi-antenna snapshot receiver

J. Rossouw van der Merwe, Alejandro Fernández-Dans Goicoechea, Alexander Rügamer, Daniel Rubino, Xabier Zubizarreta, and Wolfgang Felber
Fraunhofer IIS, Nuremberg, Germany
johannes.roussouw.vandermerwe@iis.fraunhofer.de

***Abstract*— A global navigation satellite system (GNSS) snapshot receiver records a snapshot of raw data and then forwards it to a server for processing. The server then sends information regarding the position and time for the receiver back to the receiver. This technology enables low-power positioning and can also be used for remote processing of encrypted signals. A multi-antenna receiver benefits from increased spatial diversity, as beamforming and nullsteering can be implemented. Both these technologies improve receiver robustness against interferences, multipath effects and spoofing. A snapshot receiver with a six-element antenna array is presented. Data is captured with a multi-channel recorder, from which snapshots are extracted and processed. GNSS acquisition algorithms which use the channels coherently, incoherently, and a mixture of both (first estimate the steering-weights and then to combine coherently), are evaluated and presented. The results are compared to a single channel snapshot which has an equal snapshot data-size. Results show that with small snapshots, a single channel has superior performance. However, with larger snapshots similar performance is achieved, as what is theoretically expected, but further providing the potential advantage of spoofing detection and interference mitigation.**

***Index Terms*—Global navigation satellite system (GNSS), beamforming, server based processing, antenna array.**

I. Introduction

Server-based global navigation satellite system (GNSS) processing allows for the remote evaluation of GNSS signals, as what is observed by a receiver. This is commonly referred to as snapshot processing, as a small snapshot of raw sample data is sent from the receiver to the server for processing [1], [2]. The server will then compute the position, velocity, and time (PVT) solution of the snapshot, and return it to the receiver. The main aim of this technique is to remove processing burden from the receiver and transfer it to a server.

Server-based processing can be applied to low-power devices [3], [4], which do not require a full GNSS receiver for positioning. This saves on power and weight requirements for the receiver as well as the associated system, hence, it is often used for low size, weight and power (SWAP) devices. Applications such as remote sensing and animal tracking can benefit from this technique. Mobile devices can also profit from this approach [5].

Spoofing, the transmission of false signals to manipulate a receiver, is a concern for GNSS receivers [6]. Encrypted GNSS signals are secure against spoofing attacks, as the signal properties and codes are not publicly available and therefore not susceptible to be falsified. Thus, another application for server-based processing is the verification or the secure determination of a receiver's position using encrypted GNSS signals [7], [8]. Inexpensive receivers do not have the required security module for cryptographically protected GNSS signals on-board, but a central server having this outsourced security module may be used instead.

978-1-5386-9473-2/19/$31.00 ©2019 IEEE

This paper extends on current snapshot processing methods by using a receiver with an array of antennas. This allows spatial processing methods, such as beamforming and null-steering, to be implemented. Beamforming has the benefit of improving the received signal strength for each individual signal: in digital post-processing beamforming beams are formed in the direction of the origin of a signal. This increases the gain of the signal and suppresses signals from other directions. Nullsteering aims to remove signals from some directions. Interference signals deteriorate the performance of a receiver, and spoofing signals mislead the results of a receiver; therefore, nullsteering is a powerful technique to improve the robustness of a receiver by removing unwanted signals. It can therefore be concluded that by using multiple antennas, the overall performance of the snapshot can consequently be improved.

The drawback of using multiple antennas, besides the larger antenna size, is that it requires multiple synchronized receiver channels. This increases system complexity and costs, which makes this technique counter productive for low SWAP devices. The focus of this paper is to establish the benefit of beamforming in relation to the added infrastructure costs, and to compensate for the increased number of snapshots–one per antenna element. The paper presents the results obtained with an experimental prototype. This will establish a baseline for future projects. This work will enhance the robustness of snapshot receivers by exploiting the spatial domain.

A background on snapshot receivers and server based processing is provided in Section II. An introduction to beamforming with multiple antennas is given in Section III. The implementation of beamforming methods to a snapshot receiver is presented and the advantages and disadvantages are discussed in Section IV. The experimental setup is introduced in Section V, and results are presented in Section VI, and the conclusions are drawn in Section VII.

II. Snapshot receivers

A conventional GNSS receiver starts with acquisition to find satellite signals and estimates an initial carrier Doppler and code phase for them [9]. These values are then used

to initialize a tracking channel, which refines the estimates through the use of tracking loops. The output of the tracking channels are then used to extract the encoded navigation message, to determine the pseudoranges to each satellite, and finally to compute the PVT solution of the receiver.

A snapshot receiver in comparison only has a snapshot of a few milliseconds of raw sample data to work with [1]. Hence, it can only achieve acquisition, as there is not enough data available for a tracking process, nor sufficient data to obtain the navigation message. Since the ephemeris data cannot be decoded, this data is obtained from a secondary source. A direct pseudorange cannot be derived from the acquisition results since the time transmission of the satellite is not available; however, given an appropriate estimate receiver position and time, together with external ephemeris data, the pseudorange can be reconstructed [10]. The PVT computation is therefore altered to allow this form of positioning.

As acquisition forms the base of the entire processing chain (not just for initialization like with a conventional receiver), it is important to have high performance algorithms. The recorded data of the receiver is transmitted via a data-link to the server. Therefore, the snapshot length and quantization is often reduced to satisfy data transmission limitations. This is a trade-off for the receiver [7], as the smaller the snapshot the poorer the acquisition performance is [11].

III. Beamforming with an antenna array

An antenna array consists of two or more antennas used together, and can allow electronic steering of the antenna pattern [12]. A beam can be generated by altering the phase and gain of each antenna. These gain and phase values are collectively referred to as the steering vector. In the case of beamforming it is often also referred to as the beamforming weights. The different phase values represent the delay of the electromagnetic (EM) wave. As each antenna has a different position relative to the others, different delays (i.e. phases) are observed for signals originating form different directions. The array can steer in both transmitting and receiving configurations. In the case of a receiving, the received signals are combined using the beamforming weights. Further, a receiver beam can be generated for each satellite independently.

To achieve beamforming an array of antennas is required. The positions of the antennas relative to each other should be known, and the array should be calibrated [13]. Each receiving channel should by synchronized in both frequency and time, to ensure that the array elements are used coherently.

IV. Beamforming with snapshots

Different algorithms to improve acquisition with multiple antenna elements are considered with their block diagrams shown in Fig. 1 and discussed in more detail in each subsection.

A. Conventional beamforming

Fig. 1a shows the conventional pre-correlation beamforming approach, where a beam is formed digitally from N-receiver

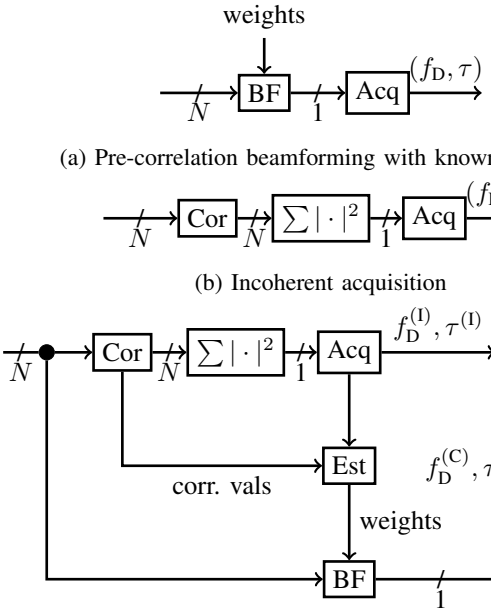

(a) Pre-correlation beamforming with known weights

(b) Incoherent acquisition

(c) Coherent acquisition with blind estimation

Fig. 1: Block diagram of different acquisition approaches

channels for each satellite before acquisition. This is denoted by the blocks "BF" for beamforming, and "Acq" for acquisition. If a satellite was acquired, then the carrier Doppler (f_D) and code phase (τ) of the signal is given as an output. These values are used in a snapshot receiver to calculate the PVT. This method requires the beamforming weights to be known in advance, hence, the array orientation, the direction-of-arrival (DOA) of each satellite, and the array calibration table should be available. This highlights the biggest disadvantage of this method: a lot of information should be known.

The gain of this algorithm is proportional to the number of antenna elements N. The probability of detection $P_\mathrm{d}^{(\mathrm{C})}$ of the detector used in the acquisition is defined as:

$$P_\mathrm{d}^{(\mathrm{C})} = Q_{\chi'^2_{2L}(N\cdot\lambda_\mathrm{d})}\left(Q^{-1}_{\chi^2_{2L}}\left(P_\mathrm{fa}\right)\right) , \tag{1}$$

where $Q_{\chi'^2_\nu(\lambda)}(\cdot)$ is the right tail probability of a non-central chi-squared random variable with ν degrees of freedom and λ is the non-centrality parameter; $Q^{-1}_{\chi^2_\nu}(\cdot)$ is the inverse function of the right tail probability of a central chi-squared random variable with ν degrees of freedom; P_fa is the probability of false alarm used to set the detector threshold; L is the number of incoherent integration segments, N is the number of antenna elements, and λ_d is the correlation gain defined as:

$$\lambda_\mathrm{d} = C/N_0 \cdot \tau_\mathrm{int} \cdot R\left(\Delta T\right)^2 \cdot \mathrm{sinc}^2\left(\pi \cdot \Delta f \cdot \tau_\mathrm{int}\right) , \tag{2}$$

where C/N_0 is the carrier-to-noise density ratio, τ_int is the coherent integration time of the correlator, $R(\cdot)$ is the auto-correlation function (ACF) of the signal, ΔT is the code-phase error, Δf is the Doppler error of the carrier, and sinc is the sampling function.

The benefit of this method is that optimal performance can be achieved: measurement phase offsets and coupling are corrected by the calibration table, suppression of multipath components due to a beam only being formed in the direction of the satellite, and all channels are added together coherently. Being best in terms of performance this method also has the most requirements. Any errors in the information, like an out-date calibration table or an offset in the orientation, results in errors when calculating the beamforming weights, and ultimately will result in sub-optimal performance. Some self calibrating and adaptive correction algorithms do exist [13]; however, these require estimation and adaptive methods. A snapshot receiver often does not record sufficient data to allow such adaptive methods to converge sufficiently; however, this could be an interesting topic for future research. Therefore, it could be argued that this method in its simple state is nor robust nor flexible.

B. Incoherent array-acquisition

Fig. 1b shows a method to incoherently do acquisition between the antenna channels. In this case, the correlation of the replica is done for each channel separately (denoted by "Cor"), then the correlated values are added together incoherently (denoted by "$\sum |\cdot|^2$"). The correlated values are then passed to acquisition (denoted by "Acq"). The benefit of this method is that no beamforming is required, hence no prior knowledge of the signals is needed. This method is a blind algorithm, and is therefore robust against phase offsets, array misalignment and calibration offsets. However, it does not form a beam to the satellite, hence other interferences, signals and multipath components are not suppressed effectively. This method is therefore robust and simple to implement, but has reduced performance in degraded environments.

As this is an incoherent addition of the array channels, the probability of detection $P_{\mathrm{d}}^{(\mathrm{I})}$ changes to:

$$P_{\mathrm{d}}^{(\mathrm{I})} = Q_{\chi'^2_{2LN}(\lambda_{\mathrm{d}})}\left(Q^{-1}_{\chi^2_{2LN}}\left(P_{\mathrm{fa}}\right)\right) . \tag{3}$$

This will result in the same gain for the satellite of interest when compared to the method of coherently adding the channels but the noise floor and influence of interferences for this method are increased. This method is also different to normal incoherent acquisition, as the incoherent data are separated by space and not time: each channel has the same data modulated data bits, thus, resulting in fewer bit-flip issues [11].

As this method combines the values after correlation, N times more correlations are required, as compared to beamforming first. This increases processing and memory requirements for this method.

C. Blind estimation

Fig. 1c shows a hybrid method which first applies an incoherent acquisition followed by a coherent acquisition using estimated beamforming weights.

At first, a blind incoherent acquisition stage occurs for every receiver channel. The signals from every element in the array are correlated with the replica of each satellite. The absolute squared values of the correlations are added in order to estimate the code phase $\tau^{(\mathrm{I})}$ and carrier Doppler $f_{\mathrm{D}}^{(\mathrm{I})}$. If the satellite is acquired, then the beam-steering weights are estimated (denoted by "Est") with the code phase $\tau^{(\mathrm{I})}$ and carrier Doppler $f_{\mathrm{D}}^{(\mathrm{I})}$ from the incoherent acquisition. If it is not acquired, the signal from one of the elements of the array is used (i.e. beamforming is omitted). Once the coefficients are estimated, the receiver channels are weighted accordingly (denoted by "BF") and a second acquisition takes place. This time the coherent code phase $\tau^{(\mathrm{C})}$ and carrier Doppler $f_{\mathrm{D}}^{(\mathrm{C})}$ are determined.

After the second acquisition occurs, a comparison between the code phases and Doppler frequencies from the first (incoherent), and the second acquisition (coherent) takes place. If these differ too much, then the satellite is discarded. This allows a secondary test to remove false positives from acquisition.

This method has the "blind" benefit like incoherent acquisition, as presented in Section IV-B. Hence, no calibration or prior knowledge of the array orientation is required. However, due to the refinement process of the secondary acquisition, the overall system has a performance that nears coherent acquisition, as presented in Section IV-A. This algorithm is as processing intensive as the previous two methods combined. However, as processing is usually performed by a high-performance server, this is not a issue.

A limitation of the method is the estimation of the beamforming weights based upon the incoherent results. These values may contain multipath components or cross-correlation components from other signals which can obscure the estimation process. In turn, the erroneous weights may form a beam that does not sufficiently suppress these unwanted signal components. In harsh environments, where the multipath components are significant, this could be an issue.

D. Acquisition comparison

If acquisition is done on a single channel a number of subsequent epochs of data can be added coherently or incoherently [9], [14]. This is a temporal addition of epochs. In coherent acquisition the detection probabilities follow central and non-central chi-squared distributions, with a fixed $\nu = 2$ degrees of freedom and a non-centrality parameter λ proportional to the number of epochs. Further, the Doppler resolution is scaled proportionally to the number of epochs, hence, additional Doppler offsets should be tested. This is why coherent acquisition has superior detection performance and Doppler resolution. However, it is sensitive to bit-transitions. Therefore, bit-transitions should either be known or estimated. In incoherent acquisition the detection probabilities also follow central and non-central chi-squared distributions. However, with degrees of freedom ν proportional to the number of epochs, and a fixed non-centrality parameter λ. Further the Doppler resolution in this case is not scaled. Therefore, incoherent acquisition has inferior performance. However, it is robust against bit-transition, as these are removed by the

addition process. Incoherent acquisition is often preferred, due to this robustness and the fact that fewer Doppler offsets are required to be tested.

If acquisition is done with multiple channels then additional epochs of data in the spatial domain could be integrated. In the case of coherent spatial additions (i.e. beamforming like Section IV-A), the detection probabilities are similar to the coherent temporal additions. The two exceptions are that the Doppler resolution is not improved (the integration time is not increased), and that the increased problems of bit-transitions is not present. Therefore coherent spatial additions has properties that lies between the properties of coherent and incoherent temporal additions. Incoherent spatial additions (like Section IV-A), has the same performance as incoherent temporal additions.

As the integration is expanded in the spatial domain, a larger effective integration can be achieved. Receiver dynamics result in the received signal changing the code phase and carrier frequency over time. This fundamentally limits long temporal integrations, but this limitation can be overcome through spatial integration. The secondary code and bit-structure of the signal are other temporal limitations to integration. Therefore, spatially integration greatly increases the achievable sensitivity of a receiver.

An example of these four methods is shown in Fig. 2. Here, normalized noisy correlation functions of a binary phase-shift keying (BPSK) signals are shown. A single epoch of data is used as the baseline (denoted by "none"). The other three lines show coherent spatial, incoherent temporal, and coherent temporal over six epochs of data (i.e. over the same equivalent data size). The coherent temporal has improved Doppler resolution, whereas the others are similar (Fig. 2b). The noise level of the single channel is the highest, followed by incoherent temporal, and lastly coherent temporal and coherent spatial have similar noise performances (Fig. 2a). This figure illustrates the differences between spatially and temporally adding data in the acquisition phase and motives the use of beamforming method to improve acquisition methods.

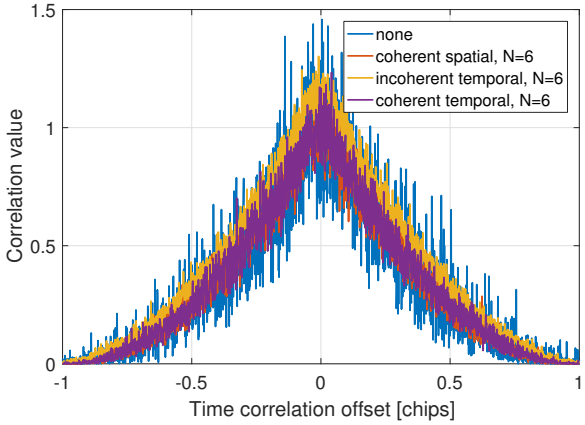

(a) Time domain comparison

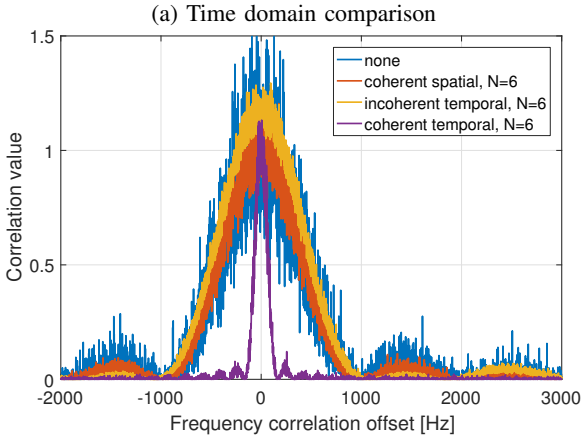

(b) Frequency domain comparison

Fig. 2: Comparison of acquisition methods

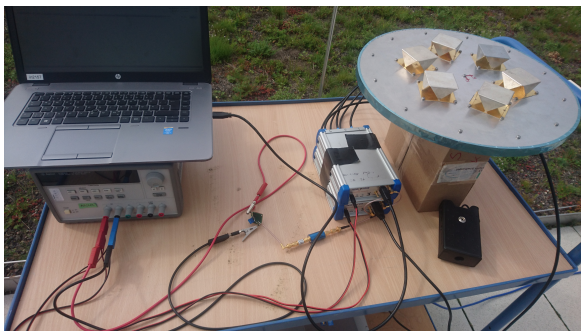

Fig. 3: Photo of the measurement system

V. Experimental setup

For the experimental setup a six element circular array is used. The array is connected to a six channel receiver which consists of 2 synchronized three channel Flexiband front-ends [15]. These front-ends use a common 10 MHz clock reference and are triggered simultaneously. They enable a maximum sample-rate of 81 MHz at 8 bit I/Q. However, for this experiment only 10.125 MHz was used. A recording of 1 min was made and saved to be used in post processing. A picture of the system is shown in Fig. 3.

The stored recordings are then interpreted by a software-defined radio (SDR) and multiple snapshots are extracted out of the original 1 min data stream. The quantization of the snapshots are reduced to 4 or 1 bit to allow smaller data sizes. The acquisition results together with PVT solution of each snapshot is stored after processing. For the processing only Global Positioning System (GPS) L1 C/A signals are considered, as this is a proof of concept. The results are then analyzed to determine the statistical performance of the different methods.

As a snapshot should be sent to a server, the data size of the snapshot should be as small as possible to minimize transmission and storage limitations. Therefore, for this study it is chosen that the snapshots are compared such that they have the same data-size. Theoretically, each snapshot should have the same amount of information, ergo, similar performance should be expected. For this experiment a snapshot-batch (B_s)

is defined as 1 ms of data sampled at 10.125 MHz 4 bit I/Q for 6 channels. The equivalent storage size of a snapshot-batch (B_s) is 60.75 kBytes. Snapshot sizes that relate to 1 B_s to 6 B_s kBytes are taken and evaluated. The following four acquisition types are made for each snapshot size:

- **NBF = no beamforming**: Only one antenna is used, i.e. only the first channel. Therefore 1 B_s relates to 6 ms of channel 1 data. 4 bit I/Q quantization is used.
- **BBF = blind beamforming**: All 6 antennas are used, therefore 1 B_s relates to 1 ms of data per channel. 4 bit I/Q quantization is used. This method uses the blind beamforming acquisition as what is presented in Section IV-C.
- **1BF = 1-bit blind beamforming**: All 6 antennas are used, but it is re-quantized to 1 bit I/Q. Therefore 1 B_s relates to 4 ms of data per channel. This method also uses the blind beamforming acquisition as what is presented in Section IV-C.
- **PBF = pre-calculated beamforming**: All 6 antennas are used, therefore 1 B_s relates to 1 ms of data per channel. 4 bit quantization is used. This method uses the beamforming acquisition as what is presented in Section IV-A. The beamforming weights are calculated according to the satellite position, the calibration table of the array, the orientation of the array, and the initial phase offset of the receiver.

The coherent time interval (1 epoch of data) for each acquisition is selected to be 1 ms, as this is equal to the code length of the signals. If more data is used, multiple epochs are added together incoherently. Two methods are used:

- **No zero padding (ZP = 0)**: The maximum number of incoherent epochs that do not require zero padding of the snapshot, i.e. K = (snapshot length) / (1 ms) - 1
- **Zero padding (ZP = 1)**: The snapshots are zero padded, i.e. K = (snapshot length) / (1 ms)

A total of 1000 snapshots are extracted and evaluated for each test. This allows sufficient statistical analysis to be done. PVT results that have a larger position error than 10 km from the reference position are omitted as this represents a complete fail of the PVT. These errors are associated with one or more false acquisitions. The percentage of failed PVTs are recorded, as these are omitted for the calculation of the statistics. The average position error and the circular error probable (CEP) of the PVT results are compared. The average number of satellites in view that are used for the PVT, along with the average peak to next peak (P2NP) for detection metric are presented. The probability that a false acquisition was made (i.e. false code and carrier was determined), for valid PVT solutions is also calculated.

VI. Results

Table I shows the percentage of failed PVTs and the number of false acquisitions. For no beamforming (NBF) and 1 bit beamforming (1BF) no PVTs where excluded, which indicates a high degree of reliability. With the beamforming methods (BBF and PBF) a more than half of the PVTs failed for $B_s = 1$, but the success rapidly improves as the snapshot size B_s increases. This is due to the fact that with a single epoch of data, bit flip issues and coherent integration is a significant limitation of the acquisition algorithm.

TABLE I: Success results

Mode		Number of failed PVTs [%]				Prob. of false acq. [‰]			
B_s	ZP	NBF	BBF	1BF	PBF	NBF	BBF	1BF	PBF
1	1	0	57.5	0	51.5	0	0.03	0	8.63
2	0	0	1.9	0	0.1	0	0.06	0	1.53
2	1	0	1.9	0	0.4	0	0.03	0	1.34
3	0	0	0.1	0	0	0	0.03	0	0.25
3	1	0	0.3	0	0	0	0	0	0.13
4	0	0	0	0	0	0	0	0	0.03
4	1	0	0	0	0	0	0	0	0.06
5	0	0	0	0	0	0	0	0	0
5	1	0	0	0	0	0	0.03	0	0.03
6	0	0	0	0	0	0	0.03	0	0
6	1	0	0	0	0	0	0	0	0

Valid PVT solution can often still be calculated even though a number of false acquisition are made. A single false acquisition may result in a large PVT error, which degrades the result significantly. For no beamforming (NBF) and 1 bit beamforming (1BF), no false acquisitions were made with valid PVTs. For the pre-calculated beamforming weights (PBF), the most false acquisition were observed (maximum was 8.63 ‰). This shows that the double acquisition stage with carrier and code comparison to remove false positives significantly reduces false acquisitions. However, it is not perfect as a maximum of 0.06 ‰) errors where still observed in the blind beamforming BBF method.

Table II shows the acquisition results for the signals. In general as the snapshot size B_s increase, so does the average number of detected satellites and the P2NP detection metric also increase. This is as expected by theory.

TABLE II: Acquisition results

Mode		Satellites in view				P2NP [dB]			
B_s	ZP	NBF	BBF	1BF	PBF	NBF	BBF	1BF	PBF
1	1	7.20	4.07	6.46	4.30	8.36	8.57	13.13	7.65
2	0	8.50	5.26	7.63	6.42	8.88	11.57	13.23	9.38
2	1	8.43	5.14	7.53	6.82	8.90	12.08	13.17	9.35
3	0	8.82	6.28	8.16	7.96	9.28	12.48	13.15	9.84
3	1	8.81	6.10	8.09	8.34	9.26	12.72	13.11	9.69
4	0	8.93	6.91	8.33	8.82	9.57	12.94	13.32	10.17
4	1	8.91	6.87	8.23	9.09	9.55	12.95	13.32	10.06
5	0	8.93	7.40	8.35	9.43	9.79	13.21	13.53	10.38
5	1	8.91	7.28	8.27	9.60	9.78	13.25	13.52	10.29
6	0	8.92	7.78	8.38	9.92	9.97	13.39	13.68	10.48
6	1	8.91	7.58	8.32	9.98	9.96	13.41	13.65	10.46

Table III shows the results for the snapshot receiver with different settings. As the integration time (relates to the snapshot length) increases: the CEP improves, the average number of detected satellites increases, and the average P2NP increases, for all acquisition methods. This is as expected by theory. The average position error converges to an error of 3.5 m, this may be due to an error between the antenna position and the reference position, the tropospheric correction

or the ionospheric model used. As this is fairly constant for all settings it can be assumed to be a constant offset.

TABLE III: Position results

Mode		Average Error [m]				CEP [m]			
B_s	ZP	NBF	BBF	1BF	PBF	NBF	BBF	1BF	PBF
1	1	3.74	4.51	3.18	4.63	11.35	125.48	11.13	89.85
2	0	3.85	4.29	3.91	3.47	4.53	71.15	3.33	18.06
2	1	3.89	4.11	3.76	4.72	4.41	63.63	3.47	16.66
3	0	3.82	3.19	3.96	3.66	3.58	18.99	2.81	6.91
3	1	3.81	3.67	3.89	3.72	3.54	24.16	2.85	6.48
4	0	3.78	3.50	3.92	3.65	3.10	6.08	2.47	5.42
4	1	3.74	3.81	3.88	3.52	3.09	6.93	2.51	5.14
5	0	3.80	3.94	3.92	3.46	2.84	5.33	2.29	4.76
5	1	3.77	3.85	3.86	3.49	2.82	5.42	2.32	4.66
6	0	3.83	4.03	3.89	3.46	2.61	4.61	2.18	4.37
6	1	3.80	3.99	3.85	3.45	2.59	3.64	2.21	4.29

In general with zero padding (ZP = 1) yields better results. This is due to the fact that a larger effective integration time and gain is achieved. This is the most evident in the small snapshot cases (e.g. $B_s = 2$), as in these cases the beamforming data uses 2 ms of data with three integration epochs instead of just using two integration epochs. Of these three epochs, one epoch would have the full integration time of 1 ms, whereas the other two would be partially filled. Combined, these two partially filled epochs result in a full epoch. Therefore, the full 2 ms of data is used for acquisition. This shows that the selection of the acquisition algorithm has a significant influence to the performance.

With small snapshots ($B_s = \{1, 2, 3\}$) no beamforming (NBF) has superior results to the beamforming methods (BBF and PBF). This is due to the fact that with small snapshots the temporal integration length is severely limited in the beamforming case. As an example, for $B_s = 1$ the no beamforming (NBF) has a single snapshot of length 6 ms, which guarantees 5 full data bits of 1 ms. This means that a guaranteed minimum of 83 % of the integration time is usable. In comparison, the beamforming cases have six channels with a length of 1 ms each which has a more than likely chance of having a a bit-flip and will have 2 partially filled epochs. This significantly reduces the usable data for acquisition. However, more complicated acquisition methods could be implemented to improve the performance for such small snapshots. With large snapshots ($B_s = \{4, 5, 6\}$) both the no beamforming (NBF) and beamforming (BBF and PBF) methods converge to have similar performances (CEP $\approx 3 \ldots 4$ m). This is as expected by the theory, as the amount of information contained in the snapshots are the same, hence similar performance should be achieved.

The pre-calculated beamforming (PBF) has improved CEP results in comparison the the blind beamforming algorithm (BBF), the only exception is $B_s = 6, \text{ZP} = 1$. This is as expected, as the blind algorithm is susceptible to multi-path effects. This is due to the fact that the beamforming weights are calculated after acquisition, which means that any estimation errors in acquisition are also included in the beamforming weights. The PBF also has more average satellites in view. This is also as expected: as the beamforming is done before acquisition, multipath effects are suppressed and gain is achieved before further processing. Sub 10 m precision is achieved at $B_s = 3$ for pre-calculated beamforming (PBF), and at $B_s = 4$ for blind beamforming (BBF). Therefore, for the presented data batch size of $B_s = 4$ (i.e. 4 ms snapshots from 6 antennas) is recommended for the beamforming methods.

The best positioning results are achieved by the 1 bit quantized data (1BF). This method achieved sub 10 m precision at a $B_s = 2$ (8 ms snapshots). This data has a snapshot that is four times longer compared to the beamforming methods with the same B_s. The increase in integration time benefits the position accuracy and performance. However, the number of satellites is view are not significantly increased. This may be due to dynamic range limitations and quantization losses. This shows that snapshot length vs. quantization is an important trade-off to consider in snapshot size optimization.

As a summary, the beamforming (PBF and BBF) and no beamforming (NBF) results converge for large snapshots. This is as expected by theory, and validates that the implementation of the beamforming is done correctly. This establishes that as a minimum similar performance can be achieved. Other benefits like DOA estimation or orientation estimation has not been considered, but it does build upon the current work. The acquisition algorithms selected have a significant effect on the performance, for example, it can improve false acquisitions or how much information can be used in small snapshots. To optimize performance these should be considered in detail. The integration time, whether coherent or incoherent, significantly influences the performance of the snapshot receiver. The longest possible snapshot should therefore be taken to achieve best performance. However, this also increases transmission requirements between the receiver and the server. For the presented data and algorithms 4 ms snapshots from 6 antennas is recommended.

VII. Conclusion

A six element snapshot receiver with both spatially coherent and incoherent acquisition methods was presented. The concept is intended to improve the security and robustness of snapshot processing. Comparisons with and without beamforming on snapshots with the same data size has been carried out to compare the benefits of implementing beamforming.

For small snapshots the results have shown that beamforming does not perform adequately. However, this is largely contributed to the weaknesses in the acquisition algorithm with short temporal signals. With larger snapshots (e.g. 4 ms per channel), the performance with and without beamforming converges, showing that with the same amount of information the same performance can be achieved. This is as expected by the theory. The snapshot length, i.e. achievable integration time, significantly influences the performance of the beamforming algorithms.

A blind beamforming method was presented. The benefit of this algorithms is that no prior knowledge of the antenna array is required, but it is susceptible to multipath and estimation errors. Compared to conventional beamforming algorithms,

this blind algorithm is simpler to implement but has slightly poorer results. This shows that this algorithm is suitable to introduce beamforming as an additional solution to a robust low cost snapshot receivers.

As this study demonstrates the initial combination of array processing with snapshot receivers, there are a number of possible future research topics. These include topics such as improving the acquisition methods, implementing interference mitigation using nullsteering, implementation of anti-spoofing methods like spoofing detection and spoofing mitigation, and development of orientation estimation of the array.

REFERENCES

[1] I. Fernández-Hernández and K. Borre, "Snapshot positioning without initial information," *GPS Solutions*, vol. 20, no. 4, pp. 605–616, Oct 2016. [Online]. Available: https://doi.org/10.1007/s10291-016-0530-4

[2] S. V. Shafran, E. A. Gizatulova, and I. A. Kudryavtsev, "Snapshot technology in GNSS receivers," in *2018 25th Saint Petersburg International Conference on Integrated Navigation Systems (ICINS)*, May 2018, pp. 1–3.

[3] T. N. Dinh and V. La The, "A novel design of low power consumption GPS positioning solution based on snapshot technique," in *2017 International Conference on Advanced Technologies for Communications (ATC)*, Oct 2017, pp. 285–290.

[4] B. Wales, L. Tarazona, and M. Bavaro, "Snapshot positioning for low-power miniaturised spaceborne GNSS receivers," in *2010 5th ESA Workshop on Satellite Navigation Technologies and European Workshop on GNSS Signals and Signal Processing (NAVITEC)*, Dec 2010, pp. 1–6.

[5] A. Rügamer, D. Rubino, X. Zubizarreta, W. Felber, J. Wendel, and D. Pfaffelhuber, "Spoofing resistant UAVs," in *Proceedings of the International Technical Meeting of The Satellite Division of the Institute of Navigation (ION GNSS+ 2018)*, 2018.

[6] J. R. van der Merwe, X. Zubizarreta, I. Lukčin, A. Rügamer, and W. Felber, "Classification of spoofing attack types," in *2018 European Navigation Conference (ENC)*, May 2018, pp. 91–99.

[7] D. Rubino, A. Rügamer, I. Lukčin, S. Taschke, M. Stahl, and W. Felber, "Galileo PRS snapshot receiver with serverside positioning and time verification," in *Proceedings of DGON POSNAV 2016*, 2016.

[8] A. Rügamer, D. Rubino, I. Lukčin, S. Taschke, M. Stahl, and W. Felber, "Secure Position and Time Information by Server Side PRS Snapshot Processing," in *Proceedings of the 29th International Technical Meeting of the Satellite Division of the Institute of Navigation (ION GNSS+ 2016)*, September 2016, pp. 3002–3017.

[9] E. D. Kaplan and C. J. Hegarty, *Understanding GPS: Principles and Applications*, 2nd ed., 2006.

[10] F. van Diggelen, *A-GPS: Assisted GPS, GNSS, and SBAS*. Artech House, 2009.

[11] D. Borio, C. O'Driscoll, and G. Lachapelle, "Composite GNSS signal acquisition over multiple code periods," *IEEE Transactions on Aerospace and Electronic Systems*, vol. 46, no. 1, pp. 193–206, Jan 2010.

[12] F. T. Ulaby, E. Michielssen, and U. Ravaioli, *Fundamentals of Applied Electromagnetics*. Pearson Education, 2014.

[13] E. Tuncer and B. Friedlander, *Classical and Modern Direction-of-Arrival Estimation*. Burlington: Elsevier, 2009.

[14] D. Borio, "A Statistical Theory for GNSS Signal Acquisition," 2008.

[15] A. Rügamer, F. Förster, M. Stahl, and G. Rohmer, "A Flexible and Portable Multiband GNSS Front-end System," in *Proceedings of the 25th International Technical Meeting of the Satellite Division of the Insitute of Navigation, ION GNSS 2012, September 17-21, 2012, Nashville, Tennessee, USA*, September 2012.